

Nucleon electromagnetic form factors and electroexcitation of low-lying nucleon resonances in a light-front relativistic quark model

I. G. Aznauryan^{1,2} and V. D. Burkert¹

¹*Thomas Jefferson National Accelerator Facility, Newport News, Virginia 23606, USA*

²*Yerevan Physics Institute, 375036 Yerevan, Armenia*

(Received 30 January 2012; published 8 May 2012)

We utilize a light-front relativistic quark model (LF RQM) to predict the $3q$ core contribution to the electroexcitation amplitudes for $\Delta(1232)P_{33}$, $N(1440)P_{11}$, $N(1520)D_{13}$, and $N(1535)S_{11}$ up to $Q^2 = 12 \text{ GeV}^2$. The parameters of the model have been specified via description of the nucleon electromagnetic form factors in the approach that combines $3q$ and pion-cloud contributions in the LF dynamics.

DOI: [10.1103/PhysRevC.85.055202](https://doi.org/10.1103/PhysRevC.85.055202)

PACS number(s): 12.39.Ki, 13.40.Gp, 13.40.Hq, 14.20.Gk

I. INTRODUCTION

In the past decade, with the advent of a new generation of electron beam facilities, there has been dramatic progress in studies of the electroexcitation of nucleon resonances that resulted in more reliable extractions of resonance electrocouplings and a significant extension of the Q^2 range. The most accurate and complete information has been obtained for the four lowest excited states, which have been measured in a range of Q^2 up to 8 GeV^2 for $\Delta(1232)P_{33}$ and $N(1535)S_{11}$ and up to 4.5 GeV^2 for $N(1440)P_{11}$ and $N(1520)D_{13}$ (see reviews [1,2]).

At relatively small Q^2 , nearly massless pions generate pion-loop contributions that may significantly alter quark model predictions. It is expected that the corresponding hadronic component, including contributions from other mesons, will rapidly lose strength with increasing Q^2 . The Jefferson Laboratory 12-GeV upgrade will open up a new era in the exploration of excited nucleons when the quark core of the nucleon and its excited states will be more fully exposed to the electromagnetic probe.

The aim of this paper is to estimate the $3q$ core contribution to the electrocoupling amplitudes of $\Delta(1232)P_{33}$, $N(1440)P_{11}$, $N(1520)D_{13}$, and $N(1535)S_{11}$. The approach we use is based on light-front (LF) dynamics, which presents the most suitable framework for describing the transitions between relativistic bound systems [3–5]. In early works by Berestetsky and Terent'ev [4], the approach was based on the construction of the generators of the Poincaré group in the LF. It was later formulated in the infinite momentum frame (IMF) [6,7]. This allowed one to demonstrate more clearly that diagrams which violate impulse approximation (i.e., the diagrams containing vertices like $\gamma^* \rightarrow q\bar{q}$) do not contribute. The interpretation of results for $\gamma^*N \rightarrow N(N^*)$ in terms of the vertices $N(N^*) \leftrightarrow 3q$ and corresponding wave functions became more evident. In Refs. [7–10], the LF RQM formulated in IMF was utilized for the investigation of nucleon form factors and the electroexcitation of nucleon resonances. These observables were investigated also in the LF Hamiltonian dynamics in Ref. [11]. In both cases a complete orthogonal set of wave functions has been used that corresponds to the classification of the nucleon and nucleon resonances within the group $SU(6) \times O(3)$; the relativistic-covariant form of these

wave functions has been found in Ref. [7]. We specify the parameters of the model for the $3q$ contribution via description of the nucleon electromagnetic form factors by combining the $3q$ and pion-cloud contributions. The pion-cloud contribution has been incorporated using the LF approach of Ref. [12].

In Sec. II we present briefly the formalism to compute the $3q$ contribution to the $\gamma^*N \rightarrow N(N^*)$ amplitudes. In Sec. III we discuss the description of nucleon electromagnetic form factors at $0 \leq Q^2 < 16 \text{ GeV}^2$. To achieve description of experimental data at $Q^2 > 0$, we incorporate the Q^2 dependence of the constituent quark mass that is expected from the lattice QCD and Dyson-Schwinger equations approach [13–15]. With the LF RQM specified via description of the nucleon electromagnetic form factors, we predict in Sec. IV the quark core contribution to the electroexcitation amplitudes of the aforementioned resonances at $Q^2 \leq 12 \text{ GeV}^2$. The results are summarized in Sec. V.

II. QUARK CORE CONTRIBUTION TO TRANSITION AMPLITUDES

The $3q$ contribution to the $\gamma^*N \rightarrow N(N^*)$ transitions has been evaluated within the approach of Refs. [7,8] where the LF RQM is formulated in the IMF. The IMF is chosen in such a way that the initial hadron moves along the z axis with the momentum $P_z \rightarrow \infty$, the virtual photon momentum is $k^\mu = (\frac{m_{\text{out}}^2 - m_{\text{in}}^2 - Q^2}{4P_z}, \mathbf{Q}_\perp, -\frac{m_{\text{out}}^2 - m_{\text{in}}^2 - Q^2}{4P_z})$, the final hadron momentum is $P' = P + k$, and $Q^2 \equiv -k^2 = \mathbf{Q}_\perp^2$; m_{in} and m_{out} are masses of the initial and final hadrons, respectively. The matrix elements of the electromagnetic current are related to the $3q$ -wave functions in the following way:

$$\begin{aligned} & \frac{1}{2P_z} \langle N(N^*), S'_z | J_{em}^{0,3} | N, S_z \rangle |_{P_z \rightarrow \infty} \\ & = 3e \int \Psi'^+(p'_a, p'_b, p'_c) Q_a \Psi(p_a, p_b, p_c) d\Gamma, \end{aligned} \quad (1)$$

where S_z and S'_z are the projections of the hadron spins on the z direction. In Eq. (1), it is supposed that the photon interacts with quark a (the quarks in hadrons are denoted by a, b, c), Q_a is the charge of this quark in units of e ($e^2/4\pi = 1/137$), Ψ and Ψ' are wave functions in the vertices $N(N^*) \leftrightarrow 3q$, p_i and p'_i

($i = a, b, c$) are the quark momenta in IMF, and $d\Gamma$ is the phase space volume. The relations between the matrix elements (1) and the $\gamma^*N \rightarrow N(N^*)$ form factors and transition helicity amplitudes are given in the Appendix.

Let \mathbf{q}_i ($i = a, b, c$) be the three-momenta of initial quarks in their center of mass system (c.m.s.): $\mathbf{q}_a + \mathbf{q}_b + \mathbf{q}_c = 0$. The sets of three-momenta in the IMF and c.m.s. of the quarks are related as follows:

$$\mathbf{p}_i = x_i \mathbf{P} + \mathbf{q}_{i\perp}, \quad \sum_i x_i = 1. \quad (2)$$

According to results of Ref. [7], obtained through relativistic-covariant transformation, the wave function Ψ is related to the wave function in the c.m.s. of quarks through Melosh matrices [16]:

$$\Psi = U^+(\mathbf{p}_a)U^+(\mathbf{p}_b)U^+(\mathbf{p}_c)\Psi_{\text{fss}}\Phi(\mathbf{q}_a, \mathbf{q}_b, \mathbf{q}_c). \quad (3)$$

Here we have separated the flavor-spin-space (Ψ_{fss}) and spatial (Φ) parts of the c.m.s. wave function. The Melosh matrices are

$$U(\mathbf{p}_i) = \frac{m_q + M_0 x_i + i\epsilon_{lm}\sigma_l \mathbf{q}_{im}}{\sqrt{(m_q + M_0 x_i)^2 + \mathbf{q}_{i\perp}^2}}, \quad (4)$$

where m_q is the quark mass and M_0 is invariant mass of the system of initial quarks:

$$M_0^2 = \left(\sum_i \mathbf{p}_i \right)^2 = \sum_i \frac{\mathbf{q}_{i\perp}^2 + m_q^2}{x_i}. \quad (5)$$

In the c.m.s. of quarks,

$$M_0 = \sum_i \omega_i, \quad \omega_i = \sqrt{m_q^2 + \mathbf{q}_i^2}, \quad \mathbf{q}_{iz} + \omega_i = M_0 x_i. \quad (6)$$

We construct the flavor-spin-space parts of the wave functions by utilizing the rules [11,17] that correspond to the classification of the nucleon and nucleon resonances within the group $SU(6) \times O(3)$.

For the final-state quarks, the quantities defined by Eqs. (2)–(6) are expressed through p'_i , \mathbf{q}'_i , and M'_0 . The phase space volume in Eq. (1) has the form

$$d\Gamma = (2\pi)^{-6} \frac{d\mathbf{q}_{b\perp} d\mathbf{q}_{c\perp} dx_b dx_c}{4x_a x_b x_c}. \quad (7)$$

To study sensitivity to the form of the quark wave function, we employ two forms of the spatial wave function,

$$\Phi_1 \sim \exp(-M_0^2/6\alpha_1^2), \quad (8)$$

$$\Phi_2 \sim \exp[-(\mathbf{q}_a^2 + \mathbf{q}_b^2 + \mathbf{q}_c^2)/2\alpha_2^2], \quad (9)$$

that were used, respectively, in Refs. [4,7,8] and [11].

III. NUCLEON

The nucleon electromagnetic form factors were described by combining the $3q$ and πN contributions to the nucleon wave function. With the pion loops evaluated according to Ref. [12], the nucleon wave function has the form

$$|N\rangle = 0.95|3q\rangle + 0.313|\pi N\rangle, \quad (10)$$

where the portions of different contributions were found from the condition that the charge of the proton is equal to unity: $F_{1p}(0) = 1$.

The values of the quark mass m_q and of the parameters $\alpha_{1,2}$ for the wave functions (8, 9) were found from the description of $\mu_p = G_{Mp}(0)$ and $\mu_n = G_{Mn}(0)$. The best results,

$$\mu_p = 2.86 \frac{e}{2m_N}, \quad \mu_n = -1.86 \frac{e}{2m_N}, \quad (11)$$

were obtained with $m_q(0) = 0.22$ GeV and

$$\alpha_1 = 0.37 \text{ GeV}, \quad \alpha_2 = 0.41 \text{ GeV}. \quad (12)$$

The quark mass $m_q(0) = 0.22$ GeV coincides with the value obtained from the description of the spectrum of baryons and mesons and their excited states in the relativized quark model [18,19].

The parameters (12) that correspond to different forms of wave functions (8) and (9) give very close magnitudes for the mean values of invariant masses and momenta of quarks at $Q^2 = 0$: $\langle M_0^2 \rangle \approx 1.35$ GeV² and $\langle \mathbf{q}_i^2 \rangle \approx 0.1$ GeV², $i = a, b, c$.

A constant value of the quark mass gives rise to rapidly decreasing form factors; for $G_{Mp}(Q^2)$ and $G_{Mn}(Q^2)$ this is demonstrated in Fig. 1. The wave functions (8, 9) increase as m_q decreases. Therefore, to describe the experimental data we

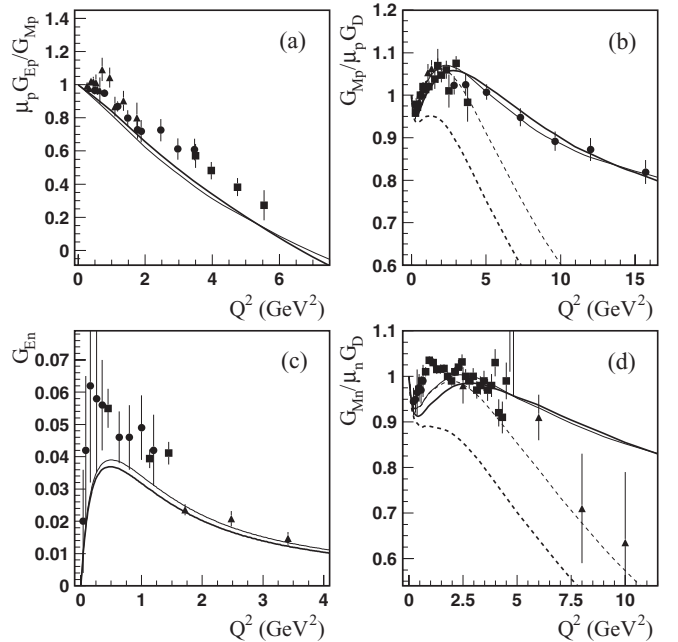


FIG. 1. Nucleon electromagnetic form factors. The curves present the results obtained taking into account two contributions to the nucleon [Eq. (10)]: the pion-cloud and the $3q$ core. The thick and thin curves correspond, respectively, to the wave functions (8) and (9). The solid curves are the results obtained with the running quark masses (13, 14) and the dashed curves correspond to the constant quark mass. Data are from the following sources: for $G_{Ep}(Q^2)/G_{Mp}(Q^2)$, Ref. [20], circles; Ref. [21], boxes; Ref. [22], triangles; for $G_{Mp}(Q^2)$, Ref. [23], circles; Ref. [24], boxes; Ref. [22], triangles; for $G_{En}(Q^2)$, Ref. [25], circles; Ref. [26], boxes; Ref. [27], triangles; and for $G_{Mn}(Q^2)$, Ref. [28], circles; Ref. [29], boxes; Ref. [30], triangles.

have assumed the Q^2 -dependent constituent quark mass. We have used two different parameterizations of this mass:

$$m_q^{(1)}(Q^2) = \frac{0.22 \text{ GeV}}{1 + Q^2/56 \text{ GeV}^2}, \quad (13)$$

$$m_q^{(2)}(Q^2) = \frac{0.22 \text{ GeV}}{1 + Q^2/18 \text{ GeV}^2}, \quad (14)$$

for the wave functions Φ_1 and Φ_2 , respectively. This resulted in a good description of the nucleon electromagnetic form factors for $Q^2 \leq 16 \text{ GeV}^2$.

Let us mention that due to strong dependence of the wave functions Φ_1 and Φ_2 on the quantities M_0^2 and $\mathbf{q}_a^2 + \mathbf{q}_b^2 + \mathbf{q}_c^2$, a slight change in the magnitude of these quantities results in a significant change in the magnitude of the predicted form factors. For example, at $Q^2 = 10 \text{ GeV}^2$, the predictions for the nucleon form factors were increased by factors 2 and 1.5 for the wave functions Φ_1 and Φ_2 , respectively. In both cases, this has been achieved by decreasing $\langle M_0^2 \rangle$ at $Q^2 = 10 \text{ GeV}^2$ from 3.1 to 2.9 GeV^2 , obtained via replacement $m_q(0) \rightarrow m_q^{(1,2)}(Q^2)$.

In Fig. 2 we show separately the pion-cloud contributions. Clearly, at $Q^2 > 2 \text{ GeV}^2$, all form factors are dominated by the $3q$ -core contribution.

The Q^2 dependence of the constituent quark mass [Eqs. (13) and (14)] is in qualitative agreement with the QCD lattice calculations and Dyson-Schwinger equations [13–15], where the running quark mass is generated dynamically. However, we want to point out that there is no direct connection between the functional forms of these masses. In QCD lattice calculations and Dyson-Schwinger equations we deal with quarks that do not possess a mass shell, and the running quark mass is a function of its virtuality, that is, the quark four-momentum square. In constituent quark models, including the

LF approaches [4,7,8,11], the quarks are mass-shell objects [see Eqs. (5) and (6)]. In LF RQM, the virtuality of quarks is characterized by invariant masses of the three-quark system: M_0^2 and $M_0'^2$. Mean values of M_0^2 and $M_0'^2$ are equal to each other and are increasing with increasing Q^2 .

The mechanism that generates the running quark mass can also generate quark anomalous magnetic moments and form factors [31]. In our approach, we have obtained a good description of the nucleon electromagnetic form factors without introducing quark anomalous magnetic moments. Introducing quark form factors results in a faster Q^2 falloff of form factors and forces $m_q(Q^2)$ to drop faster with Q^2 to describe the data. We found that descriptions that are very close to those for pointlike quarks and masses from Eqs. (13) and (14) can be obtained by introducing quark form factors

$$F_q(Q^2) = 1/(1 + Q^2/a_q)^2 \quad (15)$$

with $a_q^{(1)} > 18 \text{ GeV}^2$ and $a_q^{(2)} > 70 \text{ GeV}^2$ for the wave functions Φ_1 and Φ_2 , respectively. The corresponding quark radii are $r_q^{(1)} < r_N/5$ and $r_q^{(2)} < r_N/10$, where r_N is the mean value of the radii corresponding to $G_{Ep}(Q^2)$, $G_{Mp}(Q^2)$, and $G_{Mn}(Q^2)$. The Q^2 dependencies of quark masses for minimal values of a_q are

$$m_q^{(1)}(Q^2) = \frac{0.22 \text{ GeV}}{1 + Q^2/20 \text{ GeV}^2}, \quad (16)$$

$$m_q^{(2)}(Q^2) = \frac{0.22 \text{ GeV}}{1 + Q^2/6 \text{ GeV}^2}. \quad (17)$$

Therefore, in our approach the quark mass can be in ranges given by Eqs. (13) and (14) and Eqs. (16) and (17). As mentioned above, the results for the nucleon electromagnetic form factors obtained taking into account quark form factors [Eq. (15)] and masses [Eqs. (16) and (17)] are very close to those for pointlike quarks and masses [Eqs. (13) and (14)]. For this reason, they are not shown separately in Figs. 1 and 2.

IV. NUCLEON RESONANCES $\Delta(1232)P_{33}$, $N(1440)P_{11}$, $N(1520)D_{13}$, AND $N(1535)S_{11}$

No investigations are available that allow for the separation of the $3q$ and πN (or meson-nucleon) contributions to nucleon resonances. Therefore, the weights of the $3q$ contributions to the resonances

$$|N^*\rangle = c_{N^*}|3q\rangle + \dots, \quad c_{N^*} < 1 \quad (18)$$

are unknown. We estimate these weights by fitting to experimental $\gamma^*N \rightarrow N^*$ amplitudes. The range of Q^2 for the fit has been chosen according to available information on the possible meson-cloud contribution to the transition amplitudes. In Ref. [32], the dynamical model has been applied to describe the data on pion electroproduction on proton in the $\Delta(1232)P_{33}$ resonance region at $Q^2 \leq 4 \text{ GeV}^2$. As a result, the contribution that can be associated with the meson-cloud contribution to $\gamma^*N \rightarrow \Delta(1232)P_{33}$ has been found. Unlike for the nucleon, this contribution cannot be neglected at $Q^2 = 2 - 4 \text{ GeV}^2$ (see Fig. 3). In Ref. [44], the coupled-channel approach has been applied to the description of the pion photoproduction data, and the meson-cloud contribution to the transverse amplitudes for

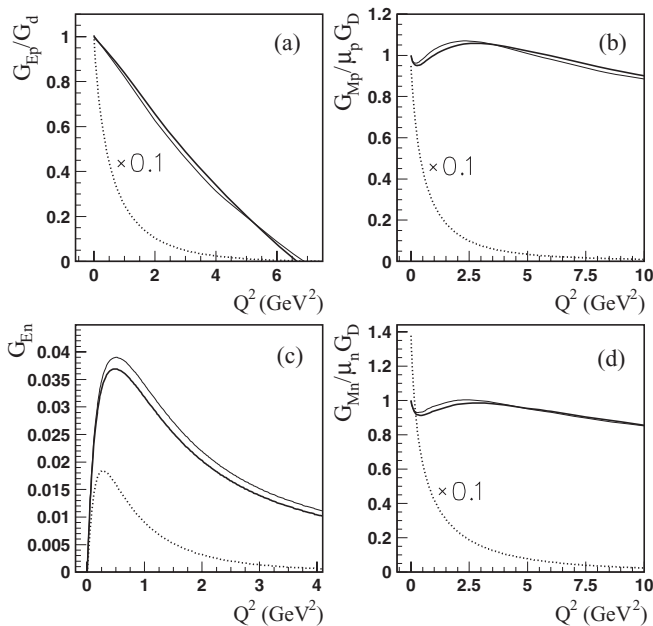


FIG. 2. Nucleon electromagnetic form factors. The legend for the solid curves is the same as for Fig. 1. The dotted curves are the pion-cloud contributions [12]; for all form factors, except $G_{E\pi}(Q^2)$, the shown results for these contributions should be multiplied by 0.1.

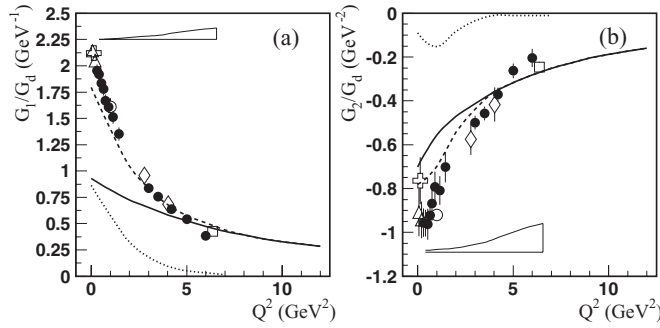


FIG. 3. The $\gamma^* p \rightarrow \Delta(1232)P_{33}$ transition form factors. The solid curves correspond to the LF RQM predictions; the weight factors for the $3q$ contributions to $\Delta(1232)P_{33}$ are $c_{N^*}^{(1)} \approx c_{N^*}^{(2)} = 0.53 \pm 0.04$ for the wave functions of Eqs. (8) and (9). The dotted curves correspond to the meson-cloud contributions obtained in the dynamical model [32]. The dashed curves present the sum of the $3q$ and meson-cloud contributions. Solid circles are the amplitudes extracted from the JLab/Hall B pion electroproduction data [33], bands represent model uncertainties of these results. The results from other experiments are denoted by open triangles [34–36], open crosses [37–39], open rhombuses [40], open boxes [41], and open circles [42,43].

the $N(1440)P_{11}$, $N(1520)D_{13}$, and $N(1535)S_{11}$ has been found at $Q^2 = 0$. The predicted Q^2 dependence of this contribution for absolute values of the amplitudes has been presented. According to these results, meson-cloud contributions to $\gamma^* N \rightarrow N(1440)P_{11}$, $N(1520)D_{13}$, and $N(1535)S_{11}$ are negligible at $Q^2 > 2 \text{ GeV}^2$. Similar results are obtained for both transverse and longitudinal $\gamma^* N \rightarrow N(1440)P_{11}$ amplitudes via estimation of the σN contribution to this transition [45] (see Fig. 4).

We therefore determine the $3q$ contribution to the resonances by fitting the experimental amplitudes at $Q^2 > 4 \text{ GeV}^2$ for $\Delta(1232)P_{33}$ and at $Q^2 = 2.5\text{--}4.5 \text{ GeV}^2$ for $N(1440)P_{11}$, $N(1520)D_{13}$, and $N(1535)S_{11}$, assuming that at these Q^2 the

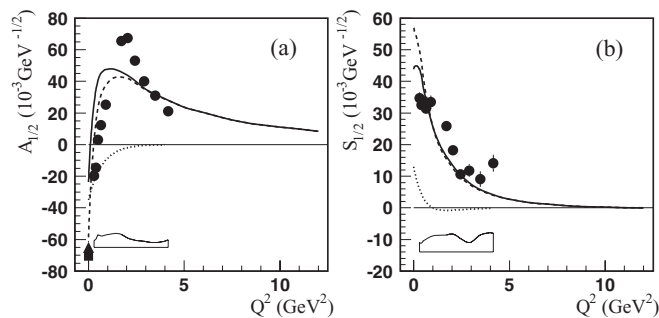


FIG. 4. The $\gamma^* p \rightarrow N(1440)P_{11}$ transition helicity amplitudes. The solid curves are the LF RQM predictions obtained with the weight factors $c_{N^*}^{(1)} = 0.73 \pm 0.05$ and $c_{N^*}^{(2)} = 0.77 \pm 0.05$ for the $3q$ contribution to the $N(1440)P_{11}$. The dotted curves correspond to the σN contribution [45]. The dashed curves present the sum of the $3q$ and σN contributions. Solid circles are the amplitudes extracted from the JLab/Hall B pion electroproduction data [33]; bands represent model uncertainties of these results. The full box at $Q^2 = 0$ is the amplitude extracted from JLab/Hall B π photoproduction data [46]. The full triangle at $Q^2 = 0$ is the RPP estimate [47].

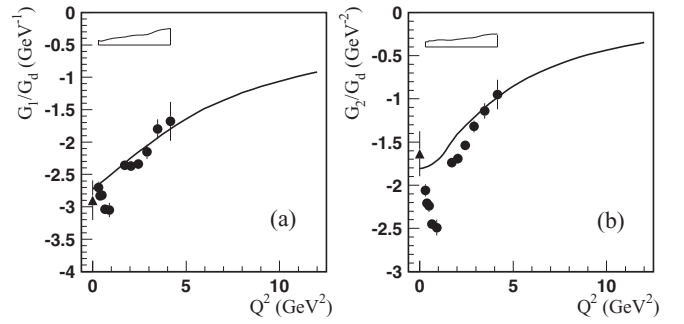


FIG. 5. The $\gamma^* p \rightarrow N(1520)D_{13}$ transition form factors. $c_{N^*}^{(1)} = 0.78 \pm 0.06$, and $c_{N^*}^{(2)} = 0.82 \pm 0.06$. Other parts of the legend are the same as for Fig. 4.

transition amplitudes are dominated by the $3q$ contribution. The results are shown in Figs. 3–6. For $\Delta(1232)P_{33}$ and $N(1440)P_{11}$, we present also the results where the $3q$ core is complemented, respectively, by the meson-cloud [32] and σN [45] contributions. These contributions significantly improve the agreement with experimental amplitudes at low Q^2 .

Here we comment on the amplitudes presented in Figs. 3–6. As shown in Refs. [9,54], there are difficulties in the utilization of the LF approaches [4,7,8,11] for hadrons with spins $J \geq 1$. These difficulties are not present if Eq. (1) is used to calculate only those matrix elements that correspond to $S'_z = J$ [9]. This restricts the number of transition form factors that can be investigated for the resonances $\Delta(1232)P_{33}$ and $N(1520)D_{13}$. As can be seen from Eqs. (A15) and (A16), the matrix elements with $S'_z = \frac{3}{2}$ relate to only two transition form factors: $G_1(Q^2)$ and $G_2(Q^2)$. Consequently, we cannot present the results in terms of transition helicity amplitudes for $\Delta(1232)P_{33}$ and $N(1520)D_{13}$, while the resonances with $J = \frac{1}{2}$, that is, $N(1440)P_{11}$ and $N(1535)S_{11}$, are presented in terms of these amplitudes.

Using Eqs. (A22)–(A27), the transition form factors $G_{1,2}(Q^2)$ for $\Delta(1232)P_{33}$ and $N(1520)D_{13}$ can be related to the transition helicity amplitudes. For $G_1(Q^2)$, the relation has

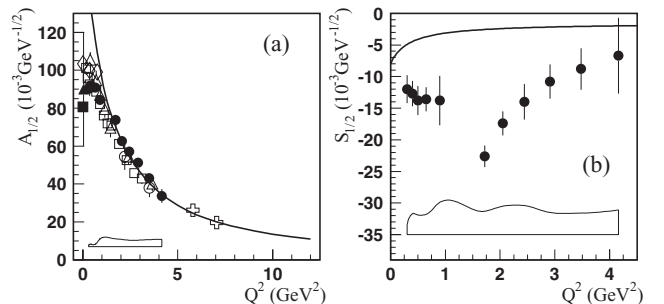


FIG. 6. The $\gamma^* p \rightarrow N(1535)S_{11}$ transition helicity amplitudes. The open triangles [48], open boxes [49], and open rhombuses [50,51] are the amplitudes extracted from the JLab/Hall B η electroproduction data; the open circles [52] and open crosses [53] are the amplitudes extracted from the JLab/Hall C η electroproduction data. $c_{N^*}^{(1)} = 0.88 \pm 0.03$, and $c_{N^*}^{(2)} = 0.94 \pm 0.03$. Other parts of the legend are the same as for Fig. 4.

a simple form,

$$G_1(Q^2) = \mp \frac{m_{N^*}}{2XQ_{\pm}} \left(A_{1/2} \pm \frac{1}{\sqrt{3}} A_{3/2} \right), \quad (19)$$

where Q_{\pm} and X are defined by Eqs. (A14) and (A24) and the upper and lower symbols correspond, respectively, to $\Delta(1232)P_{33}$ and $N(1520)D_{13}$. For $\Delta(1232)P_{33}$, it is useful to also present the following relation:

$$G_1(Q^2) = \sqrt{\frac{3}{2}} \frac{m_{N^*}(m_{N^*} + m_N)}{m_N Q_+} [G_M(Q^2) - G_E(Q^2)], \quad (20)$$

where $G_M(Q^2)$ and $G_E(Q^2)$ are the form factors defined in Ref. [55].

We note that the predictions obtained with different wave functions [Eqs. (8) and (9)] and corresponding masses [Eqs. (13) and (14)], as well as the predictions found taking into account quark form factors [Eq. (15)] and masses from Eqs. (16) and (17) differ only in the weight factors c_{N^*} for the wave functions (8) and (9); these factors are given in the figure captions. The LF RQM predictions for resonances are therefore presented by a single (thick solid) curve.

We also note that the nucleon and $\Delta(1232)P_{33}$ as well as $N(1440)P_{11}$ are considered as members of the $[56, 0^+]_R$ and $[56, 0^+]_R$ multiplets, respectively. $N(1520)D_{13}$ is taken as the state ${}^2 8_{3/2}$ of the multiplet $[70, 1^-]$ and $N(1535)S_{11}$ as a mixture of the states ${}^2 8_{1/2}$ and ${}^4 8_{1/2}$ in this multiplet:

$$N(1535)S_{11} = \cos\theta_S |{}^2 8_{1/2}\rangle - \sin\theta_S |{}^4 8_{1/2}\rangle. \quad (21)$$

Here we use the notation ${}^{2S+1}SU(3)_J$, which gives the assignment according to the $SU(3)$ group, J is the spin of the resonance, and S is the total spin of quarks. The mixing angle is taken equal to $\theta_S = -31^\circ$ as found from the hadronic decays [56,57]. The transition $\gamma^* p \rightarrow {}^4 8_{1/2}$, which is forbidden in the single-quark transition model [58], turned out very small compared to $\gamma^* p \rightarrow {}^2 8_{1/2}$ in the LF RQM too. Therefore, the $\gamma^* p \rightarrow N(1535)S_{11}$ amplitudes are determined mainly by the first term in Eq. (21).

V. SUMMARY

We have described the nucleon electromagnetic form factors in a wide range of Q^2 by complementing the $3q$ -core contribution with contribution of the pion cloud and assuming the constituent quark mass to decrease with increasing Q^2 . The pion-cloud contribution is negligible at $Q^2 > 2 \text{ GeV}^2$, but it is important to describe the neutron electric form factor and the dip in the magnetic form factors at very small Q^2 . The decreasing quark mass allowed us to compensate for the rapidly falling form factors with increasing Q^2 . The Q^2 -dependent quark mass is in qualitative agreement with results from QCD lattice and Dyson-Schwinger equations. The mechanism that generates the running quark mass within these approaches can also produce quark form factors which result in a faster falloff of the nucleon form factors. This, in turn, forces $m_q(Q^2)$ to drop faster with Q^2 in order to describe the data. From the description of the nucleon electromagnetic form factors, we have found empirically the boundaries for

the quark form factors and the corresponding boundaries for $m_q(Q^2)$.

With the LF RQM specified via description of the nucleon electromagnetic form factors, we have predicted the quark core contribution to the electroexcitation amplitudes of the resonances $\Delta(1232)P_{33}$, $N(1440)P_{11}$, $N(1520)D_{13}$, and $N(1535)S_{11}$ up to $Q^2 = 12 \text{ GeV}^2$, where the weight factor of the $3q$ contribution to the resonance occurs as the only parameter. This parameter was found by fitting to experimental amplitudes in a Q^2 range, where the meson-cloud contribution is expected to be negligible. The important feature of our predictions is the fact that at these Q^2 we describe both amplitudes investigated for each resonance by fitting a single parameter.

For $\Delta(1232)P_{33}$ and $N(1440)P_{11}$, we also present the results where the $3q$ core is complemented, respectively, by the meson-cloud contribution found in the dynamical model [32] and the σN contribution found in Ref. [45]. These contributions significantly improve the agreement with experimental amplitudes at low Q^2 .

Both effects employed in our description of electromagnetic transitions, meson-baryon contributions to N and N^* and running quark mass, will affect the masses of these states. There are only studies of the pion-cloud contributions to the nucleon mass using the cloudy bag model [59,60] and Dyson-Schwinger equations [61]. They indicate that the nucleon mass receives significant contributions from the pion loops, as much as $-(300 \div 400)$ and $-(150 \div 300)$ MeV, respectively. The investigation of the masses of N and N^* in a scheme that involves both effects is important for the development of a realistic picture of these states. Such investigation also would allow one to check the portions of the $3q$ contribution to nucleon resonances obtained in our approach empirically from the data on electroexcitation amplitudes in a Q^2 range, where this contribution is expected to be dominant.

ACKNOWLEDGMENTS

We acknowledge valuable communications with T.-S. H. Lee and C. D. Roberts. This work was supported by the US Department of Energy under Contract DE-AC05-06OR23177 and the Department of Education and Science of Republic of Armenia, Grant 11-1C015.

APPENDIX: THE RELATIONS BETWEEN THE MATRIX ELEMENTS (1) AND THE $\gamma^* N \rightarrow N(N^*)$ FORM FACTORS AND TRANSITION HELICITY AMPLITUDES

For the nucleon, the matrix elements (1) are related to the form factors in the following way:

$$\frac{1}{2P_z} \left\langle N, \frac{1}{2} \left| J_{em}^{0,3} \right| N, \frac{1}{2} \right\rangle_{P_z \rightarrow \infty} = F_1, \quad (A1)$$

$$\frac{1}{2P_z} \left\langle N, \frac{1}{2} \left| J_{em}^{0,3} \right| N, -\frac{1}{2} \right\rangle_{P_z \rightarrow \infty} = -\frac{Q}{2m_N} F_2, \quad (A2)$$

where $F_1(Q^2)$ and $F_2(Q^2)$ are the Dirac and Pauli form factors: $F_{1p}(0) = 1$, $F_{2N}(0) = \kappa_N$, the nucleon anomalous magnetic moment. The Sachs form factors are

$$G_M(Q^2) = F_1 + F_2, \quad G_E(Q^2) = F_1 - \frac{Q^2}{4m_N^2} F_2. \quad (\text{A3})$$

For the resonances with $J^P = \frac{1}{2}^\pm$,

$$\frac{1}{2P_z} \left\langle N^*, \frac{1}{2} \left| J_{em}^{0,3} \right| N, \frac{1}{2} \right\rangle_{P_z \rightarrow \infty} = Q^2 G_1, \quad (\text{A4})$$

$$\frac{1}{2P_z} \left\langle N^*, \frac{1}{2} \left| J_{em}^{0,3} \right| N, -\frac{1}{2} \right\rangle_{P_z \rightarrow \infty} \quad (\text{A5})$$

$$= \frac{\pm m_{N^*} - m_N}{2} Q G_2, \quad (\text{A6})$$

where the upper and lower symbols correspond, respectively, to $J^P = \frac{1}{2}^+$ and $\frac{1}{2}^-$ resonances, and the form factors are defined by [1,62]

$$\langle N^* | J_{em}^\mu | N \rangle \equiv e \bar{u}(P') \begin{pmatrix} 1 \\ \gamma_5 \end{pmatrix} \tilde{J}^\mu u(P), \quad (\text{A7})$$

$$\tilde{J}^\mu = (\not{k} k^\mu - k^2 \gamma^\mu) G_1 + [\not{k} \mathcal{P}^\mu - (\mathcal{P}k) \gamma^\mu] G_2, \quad (\text{A8})$$

where $\mathcal{P} \equiv \frac{1}{2}(P' + P)$, and $u(P)$, $u(P')$ are the Dirac spinors. The relations between the $\gamma^* N \rightarrow N^*$ helicity amplitudes and the form factors $G_1(Q^2)$, $G_2(Q^2)$ are following:

$$A_{\frac{3}{2}} = b[2Q^2 G_1 - (m_{N^*}^2 - m_N^2) G_2], \quad (\text{A9})$$

$$S_{\frac{1}{2}} = \pm b \frac{|\mathbf{k}|}{\sqrt{2}} \tilde{S}_{\frac{1}{2}}, \quad (\text{A10})$$

$$\tilde{S}_{\frac{1}{2}} = 2(m_{N^*} \pm m_N) G_1 + (m_{N^*} \mp m_N) G_2, \quad (\text{A11})$$

$$b \equiv e \sqrt{\frac{Q_\mp}{8m_N(m_{N^*}^2 - m_N^2)}}, \quad (\text{A12})$$

$$|\mathbf{k}| = \frac{\sqrt{Q_+ Q_-}}{2m_{N^*}}, \quad (\text{A13})$$

$$Q_\pm \equiv (m_{N^*} \pm m_N)^2 + Q^2. \quad (\text{A14})$$

For the resonances with $J^P = \frac{3}{2}^\pm$,

$$\frac{1}{2P_z} \left\langle N^*, \frac{3}{2} \left| J_{em}^{0,3} \right| N, \frac{1}{2} \right\rangle_{P_z \rightarrow \infty} = -\frac{Q}{\sqrt{2}} \left[G_1(Q^2) + \frac{\pm m_{N^*} - m_N}{2} G_2(Q^2) \right], \quad (\text{A15})$$

$$\frac{1}{2P_z} \left\langle N^*, \frac{3}{2} \left| J_{em}^{0,3} \right| N, -\frac{1}{2} \right\rangle_{P_z \rightarrow \infty} = \frac{Q^2}{2\sqrt{2}} G_2(Q^2), \quad (\text{A16})$$

and the form factors are defined by [1,62]

$$\langle N^* | J_{em}^\mu | N \rangle \equiv e \bar{u}_v(P') \begin{pmatrix} \gamma_5 \\ 1 \end{pmatrix} \Gamma^{\nu\mu} u(P), \quad (\text{A17})$$

$$\Gamma^{\nu\mu}(Q^2) = G_1 \mathcal{H}_1^{\nu\mu} + G_2 \mathcal{H}_2^{\nu\mu} + G_3 \mathcal{H}_3^{\nu\mu}, \quad (\text{A18})$$

$$\mathcal{H}_1^{\nu\mu} = \not{k} g^{\nu\mu} - k^\nu \gamma^\mu, \quad (\text{A19})$$

$$\mathcal{H}_2^{\nu\mu} = k^\nu P'^\mu - (kP') g^{\nu\mu}, \quad (\text{A20})$$

$$\mathcal{H}_3^{\nu\mu} = k^\nu k^\mu - k^2 g^{\nu\mu}, \quad (\text{A21})$$

where $u_v(P')$ is the generalized Rarita-Schwinger spinor. The relations between the $\gamma^* N \rightarrow N^*$ helicity amplitudes and form factors for the $J^P = \frac{3}{2}^\pm$ resonances are following:

$$A_{1/2} = h_3 X, \quad A_{3/2} = \pm \sqrt{3} h_2 X, \quad (\text{A22})$$

$$S_{1/2} = h_1 \frac{|\mathbf{k}|}{\sqrt{2} m_{N^*}} X, \quad (\text{A23})$$

$$X \equiv e \sqrt{\frac{Q_\mp}{48m_N(m_{N^*}^2 - m_N^2)}}, \quad (\text{A24})$$

where

$$h_1(Q^2) = \pm 4m_{N^*} G_1(Q^2) + 4m_{N^*}^2 G_2(Q^2) + 2(m_{N^*}^2 - m_N^2 - Q^2) G_3(Q^2), \quad (\text{A25})$$

$$h_2(Q^2) = -2(\pm m_{N^*} + m_N) G_1(Q^2) - (m_{N^*}^2 - m_N^2 - Q^2) G_2(Q^2) + 2Q^2 G_3(Q^2), \quad (\text{A26})$$

$$h_3(Q^2) = \mp \frac{2}{m_{N^*}} [Q^2 + m_N(\pm m_{N^*} + m_N)] G_1(Q^2) + (m_{N^*}^2 - m_N^2 - Q^2) G_2(Q^2) - 2Q^2 G_3(Q^2). \quad (\text{A27})$$

[1] I. G. Aznauryan and V. D. Burkert, *Prog. Part. Nucl. Phys.* **67**, 1 (2012).
[2] L. Tiator, D. Drechsel, S. S. Kamalov, and M. Vanderhaeghen, *arXiv:1109.6745*.
[3] S. D. Drell and T. M. Yan, *Phys. Rev. Lett.* **24**, 181 (1970).
[4] V. B. Berestetskii and M. V. Terent'ev, *Sov. J. Nucl. Phys.* **24**, 1044 (1976); **25**, 347 (1977).
[5] S. J. Brodsky and S. D. Drell, *Phys. Rev. D* **22**, 2236 (1980).
[6] L. A. Kondratyuk and M. V. Terent'ev, *Yad. Fiz.* **31**, 1087 (1980).
[7] I. G. Aznauryan, A. S. Bagdasaryan, and N. L. Ter-Isaakyan, *Phys. Lett. B* **112**, 393 (1982); *Yad. Fiz.* **36**, 1278 (1982).

[8] I. G. Aznauryan, *Phys. Lett. B* **316**, 391 (1993); *Z. Phys. A* **346**, 297 (1993).
[9] I. G. Aznauryan and A. S. Bagdasaryan, *Sov. J. Nucl. Phys.* **41**, 158 (1985).
[10] I. G. Aznauryan, *Phys. Rev. C* **76**, 025212 (2007).
[11] S. Capstick and B. D. Keister, *Phys. Rev. D* **51**, 3598 (1995).
[12] G. A. Miller, *Phys. Rev. C* **66**, 032201 (2002).
[13] P. O. Bowman, U. M. Heller, D. B. Leinweber, M. B. Parappilly, A. G. Williams, and J. Zhang, *Phys. Rev. D* **71**, 054507 (2005).
[14] M. S. Bhagwat, M. A. Pichowsky, C. D. Roberts, and P. C. Tandy, *Phys. Rev. C* **68**, 015203 (2003).

- [15] M. S. Bhagwat and P. C. Tandy, *AIP. Conf. Proc.* **842**, 225 (2006).
- [16] H. J. Melosh, *Phys. Rev. D* **9**, 1095 (1974).
- [17] R. Koniuk and N. Isgur, *Phys. Rev. D* **21**, 1868 (1980).
- [18] S. Godfrey and N. Isgur, *Phys. Rev. D* **32**, 189 (1985).
- [19] S. Capstick and N. Isgur, *Phys. Rev. D* **34**, 2809 (1986).
- [20] M. K. Jones *et al.*, *Phys. Rev. Lett.* **84**, 1398 (2000).
- [21] O. Gayou *et al.*, *Phys. Rev. Lett.* **88**, 092301 (2002).
- [22] L. E. Price *et al.*, *Phys. Rev. D* **4**, 45 (1971).
- [23] A. F. Sill *et al.*, *Phys. Rev. D* **48**, 29 (1993).
- [24] W. Bartel *et al.*, *Nucl. Phys. B* **58**, 429 (1973).
- [25] R. Schiavilla and I. Sick, *Phys. Rev. C* **64**, 041002 (2001).
- [26] R. Madey *et al.*, *Phys. Rev. Lett.* **91**, 122002 (2003).
- [27] S. Riordan *et al.*, *Phys. Rev. Lett.* **105**, 262302 (2010).
- [28] B. Anderson *et al.*, *Phys. Rev. C* **75**, 043003 (2007).
- [29] J. Lachniet *et al.* (CLAS Collaboration), *Phys. Rev. Lett.* **102**, 192001 (2009).
- [30] S. Rock *et al.*, *Phys. Rev. Lett.* **49**, 1139 (1982).
- [31] L. Chang, Y.-X. Liu, and C. D. Roberts, *Phys. Rev. Lett.* **106**, 072001 (2011).
- [32] T. Sato and T.-S. H. Lee, *Phys. Rev. C* **63**, 055201 (2001).
- [33] I. G. Aznauryan *et al.* (CLAS Collaboration), *Phys. Rev. C* **80**, 055203 (2009); **78**, 045209 (2008).
- [34] S. Stave *et al.*, *Eur. Phys. J. A* **30**, 471 (2006).
- [35] N. F. Sparveris *et al.*, *Phys. Lett. B* **651**, 102 (2007).
- [36] S. Stave *et al.*, *Phys. Rev. C* **78**, 025209 (2008).
- [37] C. Mertz *et al.*, *Phys. Rev. Lett.* **86**, 2963 (2001).
- [38] C. Kunz *et al.*, *Phys. Lett. B* **564**, 21 (2003).
- [39] N. F. Sparveris *et al.*, *Phys. Rev. Lett.* **94**, 022003 (2005).
- [40] V. V. Frolov *et al.*, *Phys. Rev. Lett.* **82**, 45 (1999).
- [41] A. N. Villano *et al.*, *Phys. Rev. C* **80**, 035203 (2009).
- [42] J. J. Kelly *et al.*, *Phys. Rev. Lett.* **95**, 102001 (2005).
- [43] J. J. Kelly *et al.*, *Phys. Rev. C* **75**, 025201 (2007).
- [44] B. Juliá-Díaz, T.-S. H. Lee, A. Matsuyama, T. Sato, and L. C. Smith, *Phys. Rev. C* **77**, 045205 (2008).
- [45] I. T. Obukhovskiy, A. Faessler, D. K. Fedorov, T. Gutsche, and V. E. Lyubovitskij, *Phys. Rev. D* **84**, 014004 (2011).
- [46] M. Dugger *et al.* (CLAS Collaboration), *Phys. Rev. C* **79**, 065206 (2009).
- [47] Particle Data Group, K. Nakamura *et al.*, *J. Phys. G* **37**, 1 (2010).
- [48] R. Thompson *et al.* (CLAS Collaboration), *Phys. Rev. Lett.* **86**, 1702 (2001).
- [49] H. Denizli *et al.* (CLAS Collaboration), *Phys. Rev. C* **76**, 015204 (2007).
- [50] I. G. Aznauryan, V. D. Burkert, H. Egiyan, K. Joo, R. Minehart, and L. C. Smith, *Phys. Rev. C* **71**, 015201 (2005).
- [51] I. G. Aznauryan, *Phys. Rev. C* **68**, 065204 (2003).
- [52] C. S. Armstrong *et al.*, *Phys. Rev. D* **60**, 052004 (1999).
- [53] M. M. Dalton *et al.*, *Phys. Rev. C* **80**, 015205 (2009).
- [54] B. D. Keister, *Phys. Rev. D* **49**, 1500 (1994).
- [55] H. F. Jones and M. D. Scadron, *Ann. Phys.* **81**, 1 (1973).
- [56] N. Isgur and G. Karl, *Phys. Lett. B* **72**, 109 (1977).
- [57] A. J. G. Hey, P. J. Litchfield, and R. J. Cashmore, *Nucl. Phys. B* **95**, 516 (1975).
- [58] V. D. Burkert, R. DeVita, M. Battaglieri, M. Ripani, and V. Mokeev, *Phys. Rev. C* **67**, 035204 (2003).
- [59] B. C. Pearce and I. R. Afnan, *Phys. Rev. C* **34**, 991 (1986).
- [60] A. W. Thomas and S. W. Wright, in *Frontiers in Nuclear Physics: From Quark-Gluon Plasma to Supernova*, edited by S. Kuyucak (World Scientific, Singapore, 1999), pp. 172–211.
- [61] C. D. Roberts *et al.*, *Eur. Phys. J. ST* **140**, 53 (2007).
- [62] R. C. E. Devenish, T. S. Eisanschitz, and J. G. Körner, *Phys. Rev. D* **14**, 3063 (1976).